

## Melting of Two-Dimensional Adatom Superlattices Stabilized by Long-Range Electronic Interactions

N. N. Negulyaev,<sup>1</sup> V. S. Stepanyuk,<sup>2</sup> L. Niebergall,<sup>2</sup> P. Bruno,<sup>2,3</sup> M. Pivetta,<sup>4</sup> M. Ternes,<sup>4,5</sup>  
F. Patthey,<sup>4</sup> and W.-D. Schneider<sup>4</sup>

<sup>1</sup>*Fachbereich Physik, Martin-Luther-Universität, Halle-Wittenberg, Friedemann-Bach-Platz 6, D-06099 Halle, Germany*

<sup>2</sup>*Max-Planck-Institut für Mikrostrukturphysik, Weinberg 2, D-06120 Halle, Germany*

<sup>3</sup>*European Synchrotron Radiation Facility, BP 220, F-38043 Grenoble Cedex, France*

<sup>4</sup>*Ecole Polytechnique Fédérale de Lausanne (EPFL), Institut de Physique de la Matière Condensée, CH-1015 Lausanne, Switzerland*

<sup>5</sup>*Max-Planck Institut for Solid State Research, Heisenbergstraße 1, D-70569 Stuttgart, Germany*

(Received 22 October 2008; published 18 June 2009)

The melting transition of Ce adatom superlattices stabilized by long-range substrate-mediated electronic interactions on Cu(111) and Ag(111) noble metal surfaces has been investigated by low-temperature scanning tunneling microscopy, density functional theory calculations, and kinetic Monte Carlo simulations. Intriguingly, owing to the interaction between Ce adatoms and substrate, these superlattices undergo two-dimensional melting to a liquid without transition through the hexatic phase. The crucial parameters for this direct solid to liquid transition are identified.

DOI: 10.1103/PhysRevLett.102.246102

PACS numbers: 68.35.Rh, 68.37.Ef

The intrinsic properties of matter radically change in reduced dimensions. For example, long-range order defines the periodic structure of a three-dimensional (3D) crystal, while a two-dimensional (2D) solid exhibits only quasi-long-range translational (or positional) order. According to the Kosterlitz-Thouless-Halperin-Nelson-Young (KTHNY) theory [1–4], a true 2D solid melts in two steps via two distinct successive phase transitions occurring at temperatures  $T_m$  and  $T_h$ , respectively. The intermediate phase, termed hexatic, is characterized by the loss of translational order as for the liquid phase and by the subsistence of a certain degree of orientational order, in contrast to the liquid isotropic phase. For the melting of a 2D solid in the presence of a substrate potential, Nelson and Halperin predicted that the existence of the hexatic phase is hindered and melting directly occurs from the solid into the liquid phase [3].

Many investigations in diverse fields have been devoted to experimentally verify the KTHNY theory (for a review, see Refs. [5,6]): molecular liquid crystal films, rare gases or molecules adsorbed on graphite, colloidal suspensions of charged submicrometric spheres, and liquid-vapor interfaces of alloys. Moreover, the melting transition in 2D has been the subject of extensive computer simulations. With the discovery of a 2D superlattice of Ce adatoms stabilized by a free 2D electron gas on a Ag(111) surface [7], a new class of model systems was created for investigation of the melting transition in two dimensions on the atomic scale.

In this Letter, we present a combined experimental and theoretical study of the solid to liquid phase transition of 2D Ce adatom superlattices on Cu(111) and Ag(111) noble metal surfaces. By variable temperature scanning tunneling microscopy (STM) measurements, self-organization and melting of a Ce superlattice on Cu(111) is observed. Density functional theory (DFT) calculations elucidate the

formation of the Ce superlattice, and kinetic Monte Carlo (KMC) simulations describe the temperature-dependent Ce adatom coordination within this 2D system. The obtained theoretical and experimental results are compared with the predictions of the KTHNY theory. Although the Ce superlattice is stabilized by long-range interaction (LRI) mediated by surface-state electrons [7–9], the substrate atomic potential determines the Ce adsorption sites, hindering the existence of the hexatic phase. Even in the liquid phase, a sixfold symmetry induced by the Cu(111) and Ag(111) surfaces persists. These results are in agreement with the melting behavior of a 2D lattice in the presence of a “fine mesh” substrate potential [3]. To the best of our knowledge, we reveal the first example of a 2D system, which undergoes the KTHNY melting scenario on a finite substrate mesh at the atomic scale.

An amount of about 0.04 monolayer [(ML), 1 ML defined as the Cu(111) surface atom density] of Ce atoms was deposited from a thoroughly degassed tungsten filament onto a well prepared Cu(111) surface held inside a low-temperature STM under ultrahigh vacuum conditions [10]. A constant current STM image of this self-assembled superstructure, acquired at a temperature  $T = 8$  K, is presented in Fig. 1(a). Well-ordered hexagonal superlattice domains are disrupted by aggregates of two or more atoms, visible as larger white protrusions. The nucleation of these small clusters probably occurs during Ce deposition and/or at defects or adsorbates on the Cu substrate. The lower inset in Fig. 1(a) shows a detail of this superlattice, characterized by a hexagonal structure with an average interatomic distance of  $\approx 1.4$  nm [11]. STM images obtained at an estimated temperature of 9 and 14 K, respectively, are shown in Figs. 1(b) and 1(c). At these higher temperatures, the Ce adatoms become more mobile on the surface, inducing a modification of the apparent contrast between

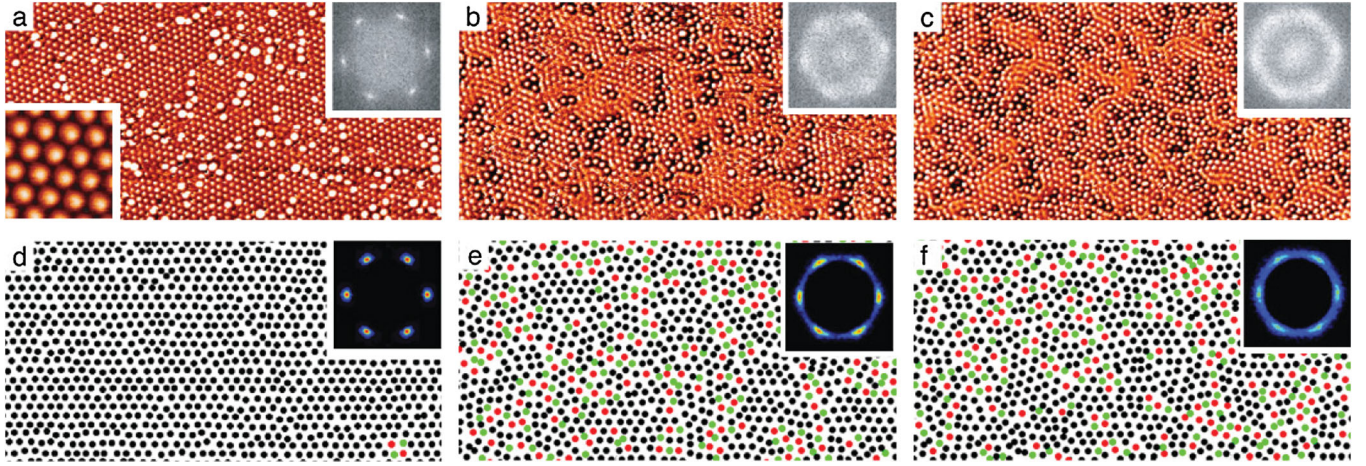


FIG. 1 (color). (a)–(c) STM images ( $75 \times 37 \text{ nm}^2$ ,  $V = -20 \text{ mV}$ ,  $I = 20 \text{ pA}$ ) acquired on Ce/Cu(111) for increasing temperatures  $T$ : (a) 8, (b) 9, and (c) 14 K. About 0.04 ML of Ce adatoms form a macroscopic-ordered superlattice with an interatomic distance of 1.4 nm, as shown in the color inset in (a) ( $9.3 \times 9.3 \text{ nm}^2$ ,  $V = +1.8 \text{ V}$ ,  $I = 20 \text{ pA}$ ). The gray-scale insets display the FT of each image. (d)–(f) Results of KMC simulations ( $55 \times 27 \text{ nm}^2$ ) for about 0.04 ML Ce on Cu(111) at (a) 9, (b) 10, and (c) 13 K. Black atoms are sixfold coordinated, red sevenfold, and green fivefold. The insets show the FT of each snapshot.

adatoms and aggregates. The gray-scale inset in Fig. 1(a) displays the 2D Fourier transform (FT), corresponding to the structure factor of the positional data acquired at 8 K. Six sharp and distinct Bragg reflections, a signature of a 2D crystalline order, are observed. At 9 and 14 K, the Bragg spots become more diffuse [see insets in Figs. 1(b) and 1(c)], and a ring appears, indicating melting of the 2D crystal. A weak hexagonal symmetry, however, is still visible in the FT.

According to the KTHNY theory, the solid, hexatic, and liquid phases can be identified in a true 2D system by a characteristic decay behavior of the density-density correlation function  $g_r(r)$  [see Eq. (1)] and the bond-angular correlation function  $g_6(r)$  [see Eq. (2)]:

$$g_r(|\mathbf{r} - \mathbf{r}'|) = \langle \exp\{i\mathbf{G}[\mathbf{u}(\mathbf{r}) - \mathbf{u}(\mathbf{r}')]\} \rangle, \quad (1)$$

$$g_6(|\mathbf{r} - \mathbf{r}'|) = \langle \exp\{i6[\theta(\mathbf{r}) - \theta(\mathbf{r}')]\} \rangle, \quad (2)$$

where  $\mathbf{G}$  denotes a reciprocal lattice vector,  $\mathbf{u}(\mathbf{r})$  is the particle displacement field, and  $\theta(\mathbf{r})$  is the angle (with respect to the  $x$  axis) of the bond centered at position  $\mathbf{r}$ . The solid phase is characterized by a quasi-long-range positional order and a long-range orientational order, corresponding to an algebraic decay for  $g_r(r)$  and to the absence of decay for  $g_6(r)$  for  $r \rightarrow \infty$ . In the hexatic phase, the positional order is only short-range [exponential decay for  $g_r(r)$ ], while the orientational order is quasi-long-range [algebraic decay for  $g_6(r)$ ]. Finally, in the liquid phase both order parameters are short-range; i.e.,  $g_r(r)$  and  $g_6(r)$  decay exponentially.

The extraction of  $g_r(r)$  from the experimental data would require a too large number of STM images for each temperature. However, from our data it was possible to compute the pair correlation function  $f(r) =$

$\langle \sum_i \sum_{j \neq i} \delta(r - |\mathbf{r}_i - \mathbf{r}_j|) \rangle$  shown in Fig. 2(a). For  $T = 8 \text{ K}$  a power-law decay  $f(r) \sim r^{-a}$ , with  $a \approx 0.9$ , was found. For  $T = 9$  and 14 K we observed an exponential decay  $f(r) \sim \exp(-br)$ , with  $b \approx 1.7$  and 1.3 nm, respectively. This finding unambiguously shows that at 8 K the system is in the solid phase, while at  $T \geq 9 \text{ K}$  the translational order is destroyed. The results for  $g_6(r)$ , deduced from the STM images of Figs. 1(a)–1(c) and summarized in Fig. 2(b), reveal that, in the solid state at  $T = 8 \text{ K}$ ,  $g_6(r)$  tends to a finite value in agreement with the prediction of the KTHNY theory. The behavior of  $g_6(r)$  for 9 and 14 K, however, is not the one expected for a true 2D system:  $g_6(r)$  approaches a constant value for large  $r$  and does not decay to zero despite the fact that the translational order is destroyed.

Therefore, an extensive theoretical investigation has been performed to clarify the 2D melting process for the Ce superlattice on Cu(111). To this end, the LRI between two single Ce adatoms at different interatomic separations was deduced using *ab initio* DFT calculations [12]. The obtained interaction potential, shown in Fig. 3, oscillates with a period of 1.4 nm, which corresponds to half of the

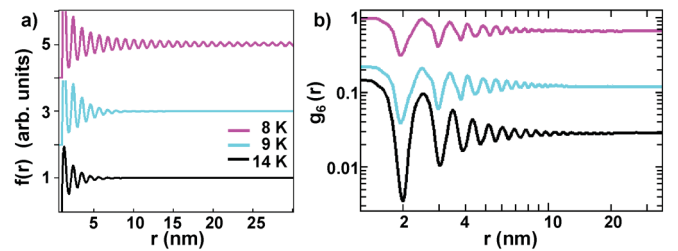


FIG. 2 (color). (a) Pair correlation function  $f(r)$  and (b) bond-angular correlation function  $g_6(r)$  extracted from the experimental data shown in Figs. 1(a)–1(c).

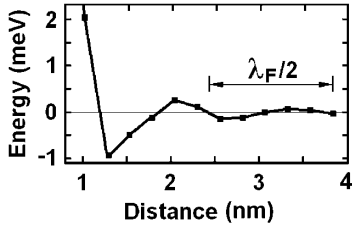


FIG. 3. Calculated long-range electronic interaction potential between two Ce adatoms on Cu(111).

surface-state electron Fermi wavelength  $\lambda_F$  on Cu(111). The first minimum of the potential exhibits a depth of about 1 meV. It is located at  $\sim 1.3$  nm, in very good agreement with the experimental finding (1.4 nm).

This calculated LRI potential was used in the large-scale KMC simulations [14,18]. The results obtained for different  $T$  are presented in Figs. 1(d)–1(f). Figure 1(d) shows a snapshot generated for  $T = 9$  K: A 2D ordered solid is formed by the Ce adatoms, as confirmed by the FT in the inset. Almost all atoms are found to be sixfold coordinated (black color code). In the KMC snapshots of Figs. 1(e) and 1(f), generated for 10 and 13 K, the number of adatoms with six nearest neighbors decreases, while the amount of sevenfold (red) and fivefold (green) coordinated atoms increases. In the FT images (see insets) a ring appears, indicating that a melting transition has taken place. However, the hexagonal symmetry persists, with a striking resemblance to the experimental data of Figs. 1(a)–1(c).

Figure 4(a) displays the density-density correlation function  $g_r(r)$  obtained for the Ce/Cu(111) 2D lattice generated by KMC simulations.  $g_r(r)$  is computed at different temperatures for  $\mathbf{G}$  corresponding to the first Bragg

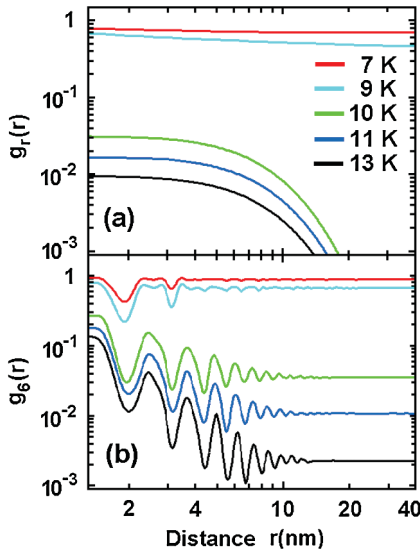


FIG. 4 (color). (a) Density-density  $g_r(r)$  and (b) bond-angular  $g_6(r)$  correlation functions calculated for about 0.04 ML of Ce on Cu(111) generated by KMC simulations.

peak of the Ce superlattice. At 7 and 9 K, the system exhibits crystalline long-range order, as  $g_r(r) \sim 1/r^\eta$ , with  $\eta = 0$  at 7 K and  $\eta = 0.09$  at 9 K. The melting of the 2D Ce lattice occurs between 9 and 10 K, since for  $T \geq 10$  K  $g_r(r)$  decays exponentially:  $g_r(r) \sim \exp(-r/\gamma)$ . The correlation length  $\gamma$  extracted for temperatures between 10 and 13 K is constant ( $\sim 3.1$  nm) within the accuracy of the calculations. This result agrees with the KTHNY theory, predicting the following dependence of the correlation length on the temperature:  $\gamma(T) = \gamma_0 \exp[C(T - T_m)^{-\nu}]$ , where  $C, \nu > 0$  [5]. This formula implies that  $\gamma(T)$  saturates at  $\gamma_0$ .

In order to detect the hexatic phase, the analysis of the bond-angular correlation function  $g_6(r)$  extracted for different temperatures and shown in Fig. 4(b) is required. In qualitative agreement with the results deduced from the experimental data,  $g_6(r)$  does not decay to zero at any  $T$  [19]. In fact, these observations are in complete agreement with the predictions of Nelson and Halperin [3]: For the melting of a 2D crystal on a fine mesh potential, (i) the existence of the hexatic phase is hindered and melting directly occurs from the solid into the liquid phase, and (ii) in the liquid phase  $g_6(r)$  tends to a finite value at large  $r$  and a substrate-induced hexagonal symmetry is present. According to the classification described in Fig. 2 of Ref. [3], the superlattice of Ce/Cu(111) is (i) a commensurate solid at 7 K [ $g_r(r) \sim 1/r^\eta$ ,  $\eta = 0$ ], (ii) a floating solid at 9 K [ $g_r(r) \sim 1/r^\eta$ ,  $\eta = 0.09$ ], and (iii) a fluid for  $T \geq 10$  K.

For a Ce superlattice on Ag(111) [7], a corresponding theoretical analysis for five different temperatures (4.0, 4.5, 4.9, 5.2, and 6.0 K) has been performed. Similar to the situation shown for Ce/Cu(111) in Fig. 4(b),  $g_6(r)$  tends to finite values; the values of  $g_6(r)$  at  $r \rightarrow \infty$  decrease from 0.61 at 4.0 K to 0.001 at 6.0 K. The melting point  $T_m$  has been found to be between 4.5 and 4.9 K. The superlattice of Ce on Ag(111) constitutes a floating solid at 4.0 ( $\eta = 0.14$ ) and 4.5 K ( $\eta = 0.18$ ) and becomes a fluid for  $T \geq 4.9$  K. The obtained values for the correlation length  $\gamma$  decrease with increasing temperature from 8.1 nm at 4.9 K to 6.0 nm at 6.0 K, indicating also saturation of  $\gamma(T)$ . These findings demonstrate that the behavior of  $g_6(r)$  is intrinsic to the Ce/Cu(111) and Ce/Ag(111) superlattices; i.e., the absence of the hexatic phase is due to the substrate potential.

The critical parameters defining the surface potential are (i) the adatom diffusion barrier  $E_D$  and (ii) the periodicity, i.e., the separation between nearest adatoms in a superlattice  $q$  with respect to the mesh density  $r_0$ . For Ce on Cu(111), the ratio between  $q \approx 1.3$  nm and  $r_0 \approx 0.256$  nm sets the relative mesh density to  $\sim 5.1$ . For Ce on Ag(111), in which  $q \approx 3.0$  nm and  $r_0 \approx 0.289$  nm [7], the ratio is  $\sim 10.4$ . In both cases, even in the liquid phase the Ce adatoms occupy discrete positions with respect to each other, and only a limited number of angles between two bonds are possible. Consequently,  $g_6(r)$  does not decay

to zero. In the limit of vanishing relative distance between neighboring adsorption sites (i.e.,  $q/r_0 \gg 1$ ), the hexatic phase appears [20].

On the other hand, the diffusion barrier height  $E_D$  describes the “flatness” of the surface. The comparison between  $E_D$  and the thermal energy of the adatom  $k_B T$  has to be considered. For  $E_D < k_B T$ , the adatom is not influenced by the substrate periodic potential, leading to diffusion on a flat surface: The adatom can be found at any point of the surface and not only in the hollow (adsorption) sites. Thus, at a typical temperature of  $T = 10$  K, with  $k_B = 0.086$  meV/K, the condition for the appearance of the hexatic phase corresponds to  $E_D < 1$  meV [20]. However, as diffusion barriers  $E_D < 1$  meV have not been observed, the hexatic phase does not exist in the considered class of 2D adatom superlattices.

In summary, Ce adatom superlattices on Cu(111) and Ag(111) undergo 2D melting without transition through the hexatic phase. A substrate-induced hexagonal symmetry is still observed in the liquid phase. The crucial parameters for the direct solid to liquid transition are (i) the diffusion barrier of a single adatom on a surface and (ii) the ratio between the interatomic separation in a superlattice and the distance between neighboring adsorption sites of the substrate lattice. The considered class of atomic superlattices exemplarily demonstrates on the atomic scale the melting of a 2D solid in the presence of a weak substrate potential.

This work was supported by Deutsche Forschungsgemeinschaft (SPP1165, SPP1153) and by the Swiss National Science Foundation.

---

[1] J. Kosterlitz and D. Thouless, *J. Phys. C* **6**, 1181 (1973).  
 [2] B.I. Halperin and D.R. Nelson, *Phys. Rev. Lett.* **41**, 121 (1978).  
 [3] D.R. Nelson and B.I. Halperin, *Phys. Rev. B* **19**, 2457 (1979).  
 [4] A.P. Young, *Phys. Rev. B* **19**, 1855 (1979).  
 [5] D.R. Nelson, in *Phase Transitions and Critical Phenomena*, edited by C. Domb and M.S. Green (Academic, London, 1983), Vol. 7, p. 1.  
 [6] K.J. Strandburg, *Rev. Mod. Phys.* **60**, 161 (1988).  
 [7] F. Sully *et al.*, *Phys. Rev. Lett.* **92**, 016101 (2004); F. Sully *et al.*, *New J. Phys.* **6**, 16 (2004); M. Ternes *et al.*, *Phys. Rev. Lett.* **93**, 146805 (2004). For Cs/Cu(111) and Cs/Ag(111), see [16].  
 [8] H. Lau and W. Kohn, *Surf. Sci.* **75**, 69 (1978); P. Hyltdgaard and M. Persson, *J. Phys. Condens. Matter* **12**, L13 (2000); J. Repp *et al.*, *Phys. Rev. Lett.* **85**, 2981 (2000); N. Knorr *et al.*, *Phys. Rev. B* **65**, 115420 (2002).  
 [9] V.S. Stepanyuk *et al.*, *Phys. Rev. B* **68**, 205410 (2003).  
 [10] R. Gaisch *et al.*, *Ultramicroscopy* **42**, 1621 (1992).  
 [11] Comparison of the orientation of the superlattice with the high-symmetry directions of the Cu(111) substrate, determined by measurements carried out before Ce deposition,

reveals a superlattice rotation of about  $30^\circ$  with respect to the substrate high-symmetry directions.

[12] Density functional theory in a local spin density approximation by means of the Korringa-Kohn-Rostocker Green’s function method for adatoms and supported clusters is used [13] (see details in [9]).  
 [13] K. Wildberger *et al.*, *Phys. Rev. Lett.* **75**, 509 (1995); V.S. Stepanyuk *et al.*, *Phys. Rev. B* **53**, 2121 (1996).  
 [14] To study atomic dynamics at different temperatures, we use the algorithm from Ref. [15] and applied in Refs. [16,17]. The Cu(111) surface is represented as a triangular lattice of equivalent fcc and hcp hollow sites with separation  $r_0/\sqrt{3}$  ( $r_0 = 0.256$  nm) between the nearest sites. The hopping rate of a Ce adatom from site  $k$  to  $j$  is computed using the formula  $v_{k \rightarrow j} = v_0 \exp(-E_{k \rightarrow j}/k_B T)$ , where  $T$  is the temperature of the substrate,  $v_0 = 10^{12}$  Hz is the attempt frequency, and  $k_B$  is the Boltzmann factor. The hopping barrier takes the form  $E_{k \rightarrow j} = E_D + 0.5(E_j - E_k)$ . Here  $E_D$  is the diffusion barrier for an isolated atom on a clean surface, and  $E_{k(j)}$  is the sum of the LRI potentials of the considered adatom with all other atoms in the system. Our *ab initio* calculations show that pairwise summation is well-justified. The binding energy of three Ce adatoms on Cu(111) placed in the corners of the equilateral triangle with a side of 1.3 nm is 10% less than the energy of the same system computed in the framework of the pairwise approach.  
 [15] K.A. Fichtorn and W.H. Weinberg, *J. Chem. Phys.* **95**, 1090 (1991).  
 [16] Th. von Hofe *et al.*, *Phys. Rev. B* **73**, 245434 (2006); M. Ziegler *et al.*, *Phys. Rev. B* **78**, 245427 (2008).  
 [17] K.A. Fichtorn and M. Scheffler, *Phys. Rev. Lett.* **84**, 5371 (2000); K.A. Fichtorn, M.L. Merrick, and M. Scheffler, *Phys. Rev. B* **68**, 041404 (2003).  
 [18] The lattice-gas KMC model can be employed, since the adatoms occupy only certain sites on the substrate. The ratio between the probabilities to find an adatom in an adsorption site and in a bridge position is determined by  $\exp(E_D/k_B T)$ , where  $E_D$  is the diffusion barrier of a single adatom. For Ce on Cu(111),  $E_D$  is estimated from our STM measurements to be  $\sim 10$  meV, leading, for a typical temperature  $T \sim 10$  K, to  $\exp(E_D/k_B T) \sim 10^5$ .  
 [19] Despite the fact that, at  $T \geq 10$  K,  $g_6(r)$  tends to a finite value, the distance between nearest adatoms changes in a diffusive fashion; i.e., the system is not a solid. In order to demonstrate this, we have calculated using KMC simulations diffusion coefficient  $D = \lim_{t \rightarrow \infty} \langle [\Delta \mathbf{u}_j(t) - \Delta \mathbf{u}_{j+1}(t)]^2 \rangle / (2t)$ , where  $\Delta \mathbf{u}(t) = \mathbf{u}(t) - \mathbf{u}(0)$ ,  $\mathbf{u}(t)$  is the particle displacement field in the moment of time  $t$ , and the indices  $j$  and  $j + 1$  refer to the neighboring adatoms. At 7 and 9 K,  $D = 0$ ; at 10 K,  $D = 0.04 \mu\text{m}^2/\text{sec}$ ; at 11 K,  $D = 0.2 \mu\text{m}^2/\text{sec}$ ; at 13 K,  $D = 1.3 \mu\text{m}^2/\text{sec}$ .  
 [20] Previous simulations for real 2D systems with dipole-dipole interaction [S.Z. Lin, B. Zheng, and S. Trimper, *Phys. Rev. E* **73**, 066106 (2006)] and Coulomb interaction [W.J. He *et al.*, *Phys. Rev. B* **68**, 195104 (2003)] indicate the presence of the hexatic phase on a continuous substrate.